

A Bayesian Approach for Selecting Relevant External Data (BASE): Application to a Study of Long-Term Outcomes in a Hemophilia Gene Therapy Trial

Tianyu Pan¹, Xiang Zhang², Weining Shen³, and Ting Ye⁴

¹Department of Pathology, Stanford University

²CSL Behring

³Department of Statistics, University of California, Irvine

⁴Department of Biostatistics, University of Washington

Abstract

Gene therapies aim to address the root causes of diseases, particularly those stemming from rare genetic defects that can be life-threatening or severely debilitating. While there has been notable progress in the development of gene therapies in recent years, understanding their long-term effectiveness remains challenging due to a lack of data on long-term outcomes, especially during the early stages of their introduction to the market. To address the critical question of estimating long-term efficacy without waiting for the completion of lengthy clinical trials, we propose a novel Bayesian framework. This framework selects pertinent data from external sources, often early-phase clinical trials with more comprehensive longitudinal efficacy data that could lead to an improved inference of the long-term efficacy outcome. We apply this methodology to predict the long-term factor IX (FIX) levels of HEMGENIX (etranacogene dezaparvovec), the first FDA-approved gene therapy to treat adults with severe Hemophilia B, in a phase 3 study. Our application showcases the capability of the framework to estimate the 5-year FIX levels following HEMGENIX therapy, demonstrating sustained FIX levels induced by HEMGENIX infusion. Additionally, we provide theoretical insights into the methodology by establishing its posterior convergence properties.

Keywords: Bayesian analysis; Data integration; Data fusion; Dynamic borrowing; Long-term effectiveness

1 Introduction

1.1 Gene therapy for Hemophilia B

Gene therapy holds great promise as a one-time treatment for life-threatening, severe-debilitating diseases such as hemophilia, with demonstrated increases in factor level expression post treatments and substantial reductions in both bleeds and utilization of factor replacement therapy in treating breakthrough bleeding (Nathwani et al., 2011, 2014; George et al., 2017; Leebeek and Miesbach, 2021). However, clinical trial participants have demonstrated variable expression in factor levels. This uncertainty has generated significant interest in understanding the long-term efficacy of gene therapy. Given the high cost of gene therapy, the potential for waning efficacy is concerning to payers who base the cost on the assumption of long-lasting effects (Kee and Maio, 2019).

Our paper aims to study the long-term efficacy of HEMGENIX, which is the first FDA-approved gene therapy designed for treating adults with severe Hemophilia B. A flourishing body of assessment reports from Health Technology Assessment (HTA) entities contribute to our understanding, including the Institute for Clinical and Economic Review (Tice et al., 2022) in the United States and the National Institute for Health and Care Excellence (Farmer et al., 2023) in the United Kingdom. The main challenge is that the data on long-term effectiveness are often lacking during the early marketing period of gene therapy, necessitating the development of appropriate methods to infer long-term effectiveness and bridge the evidence gap.

1.2 The HOPE-B Study

HOPE-B is a phase 3 study of HEMGENIX (Pipe et al., 2023, ClinicalTrials.gov number, NCT03569891) with a total of 54 male participants. At the point of our data analysis, information spanning up to 3 years post-treatment was accessible. We opted to utilize

only the data from the initial 2 years, reserving the remaining dataset for the purpose of assessing predictions. The ongoing collection of data will continue for a duration of up to 15 years as the study progresses. Due to the limited data available, both from the current study and external sources, predicting the long-term effect of the gene therapy, such as its effects after 5 years, presents a significant challenge.

In traditional clinical drug development, multiple early-phase studies (phase 1 and phase 2) are conducted before moving to a larger-scale confirmatory phase 3 study (Valentinuzzi, 2004). As a result, early-phase studies often yield data with longer observational periods. In our case, at the time of analysis, a phase 1 study of 10 patients with 5 years of follow-up (Miesbach et al., 2021) and a phase 2b study of 3 patients with 2.5 years of follow-up (Gomez et al., 2021) are crucial additional resources for inferring the long-term effect. However, it is important to note that the gene vehicle is different between the phase 1 and phase 2b/3 studies. Specifically, the phase 2b/3 studies employed the Padua gene, while the phase 1 study used a wild-type factor IX gene. These disparities could introduce systematic differences in the factor level across studies. Indeed, as shown in Figure 1(a), the phase 1 study exhibits noteworthy variations in factor levels and their longitudinal trajectories in comparison to the other two studies. This highlights the potential for biased estimates if data across the three studies are naively pooled. Throughout the rest of the paper, we designate the combined phase 2b and phase 3 study (which share substantial similarities) as our *internal study*, for which we aim to infer the long-term effect, and we consider the phase 1 study as our *external study*, from which we seek to borrow information.

Motivated by this example, a data integration method is necessary for borrowing information from the external studies (the phase 1 study) to help infer the long-term efficacy of the internal study (the phase 2b and 3 studies). Moreover, the data integration method should be designed to address the difference between the internal and external studies and guard against introducing bias into the inference of the internal studies. To achieve these

two goals, our idea consists of two key steps. First, we perform a z-transformation on both the external and internal studies, utilizing the respective mean values and standard deviations computed from the initial 10 weeks of each study. The resulting data are plotted in Figure 1(b). Following the z-transformation, the external and internal data exhibit greater similarity. Second, we augment the internal data using a selected subset of external data that exhibits similar early-stage trajectories to the internal data in order to gain efficiency of inferring long-term outcomes while guarding against introducing bias. This approach relies on the key assumption that similar initial trajectories can predict similar long-term outcomes. Furthermore, the proportion of the selected external subset offers an additional interpretation that describes the similarity between the two datasets. Specifically, a high proportion of the selected external subset would suggest greater proximity between the two datasets. In summary, the goal of the data selection procedure is to filter out irrelevant data from the external studies whilst selecting a subset that aligns with the underlying data-generating process of the internal trajectories.

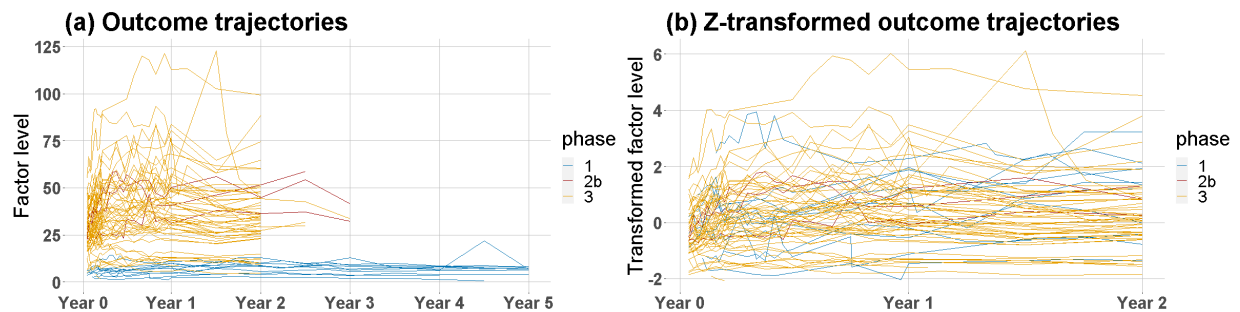


Figure 1: (a) Longitudinal outcome trajectories observed for each study. (b) The longitudinal trajectories up to the 2nd year after within-study z-transformation.

1.3 Prior work and our contributions

As mentioned in Section 1.2, the goal of combining the external and internal datasets can be perceived as a data integration problem or, more generally, as an effort to combine information from multiple data sources for an integrative and efficient inference.

Over the past decades, data integration has been an active research area. Various concepts and methods have been developed. To list a few, *data fusion* methods combine multiple datasets by assuming a shared latent variable (Liu et al., 2022) or sufficient conditional overlapping support (Li and Luedtke, 2021) for various purposes such as integrated epigenetic index estimation or average treatment effect estimation. When datasets are in matrix format, combining them can sometimes lead to block-wise missingness. To tackle this, *data integration* methods consider low-rank matrix recovery (Cai et al., 2016), spectral clustering (Park et al., 2021), and multiple block-wise imputation (Xue and Qu, 2021). *Multimodal data analysis*, where the collected data come in different types, can also be treated as a form of data selection. For example, to regress the outcome on the covariates from multiple datasets, people have considered the conventional linear regression (Li and Li, 2022) and the non-linear regression (Dai and Li, 2022). From a philosophical standpoint, Bayesian methods are natural data integration approaches. Among these, the *power prior* (Chen et al., 1999, 2000) is a notable example designed for data integration. It incorporates an uncertain discounting factor $\alpha \in [0, 1]$ into the historical likelihood to downgrade its importance while combining it with the current likelihood (Neuenschwander et al., 2009; Ibrahim et al., 2015). However, these methods downweight external data equally and do not effectively address the task of selecting relevant information from external sources. Numerous other data integration methods have emerged in diverse directions, including methods for heterogeneous treatment effect estimation (Yang et al., 2020), long-term treatment effect estimation (Athey et al., 2019; Imbens et al., 2022), doubly robust estimation for non-probability samples (Yang et al., 2020; Chen et al., 2020), and adaptive shrinkage strategy (Chen et al., 2021; Oberst et al., 2022; Hector and Martin, 2022). We refrain from an exhaustive discussion on this rapidly evolving literature and refer interested readers to the following reviews (Ritchie et al., 2015; Ibrahim et al., 2015; Hassler et al., 2023).

Despite the comprehensive developments in data integration, all the aforementioned methods either rely on incorporating the entire external information or on applying weight scaling to the whole external data to alleviate the inferential bias when conducting the data integration. We take a distinct perspective, inspired by the within-study heterogeneity observed in Figure 1(b). We propose a *data selection procedure* that selects external subsets that are similar to the internal data generating mechanism instead of integrating the entire external data or applying a universal downweighting to the entire external data. This approach recognizes that the external dataset contains heterogeneous observations, with certain data points potentially being more relevant to the internal dataset than others. To the best of our knowledge, the selection of relevant external subsets still remains an area under investigation.

The main contributions of this article are three-fold. First, we propose a novel data integration procedure, termed data selection, which has been largely overlooked till now. Our proposal is a general-purpose Bayesian data selection procedure (BASE) by assigning a prior to all possible external data subsets and using the marginal likelihood as the criteria to favor specific external subsets in the sampling process. Second, we provide theoretical justifications for our method by showing that the relevant external subset can be consistently selected with high posterior probability. Third, we introduce a novel spline model for the trend of factor level and apply BASE to the hemophilia study, producing promising results that are both statistically valid and scientifically interpretable. In comparison to the results given by the direct combination of external and internal data, and the method without external information incorporation (Shah et al., 2023), our method offers more reliable and robust conclusions about the long-term efficacy by selecting relevant external subset.

The remainder of this paper is outlined as follows. We present our methods in general terms in Section 2, and in the context of the hemophilia study in Section 3. Results from

simulation studies are in Section 4. We return to the hemophilia application in Section 5. We conclude with a discussion in Section 6. Technical proofs and pseudo-code of MCMC sampling are given in the Supplementary File.

2 A general Bayesian strategy for data selection

2.1 Method

In this section, we present a general Bayesian approach for SElecting relevant external data, which we call BASE. Specifically, we propose to select subsets from the external data that are similar to the internal data at the early stage to help infer the long-term efficacy. We will use the hemophilia study as an example to concretely describe our idea.

Suppose Y_{sit} is the outcome (i.e., factor level in our application) measured for patient i at time t in study s . The data collected from the studies are then expressed as $\{Y_{sit}, i = 1, \dots, N_s, t \in \mathcal{T}_s, s = 0, 1\}$, where N_s is the number of patients under study s , \mathcal{T}_s is the available time points for study s , and $s = 1$ indicates the internal study and $s = 0$ indicates the external study. For a model $L(\cdot | \boldsymbol{\theta}_s)$ parameterized by $\boldsymbol{\theta}_s$, our data selection procedure proceeds by first putting a prior $\Pi(\mathcal{C})$ on all the possible subsets of the external index set denoted as $\mathcal{C} \subseteq \{1, \dots, N_0\}$, and then selecting the external subsets by drawing posterior samples of \mathcal{C} given the outcomes observed before a pre-specified time T^* , namely,

$$\begin{aligned} & \Pi(\mathcal{C} | \{Y_{sit}, i = 1, \dots, N_s, t \in \mathcal{T}_s, t \leq T^*, s = 0, 1\}) \\ & \propto \underbrace{\left(\int \prod_{i=1}^{N_1} L(\{Y_{1it}\}_{t \in \mathcal{T}_1, t \leq T^*} | \boldsymbol{\theta}_1) \times \underbrace{\pi(\boldsymbol{\theta}_1 | \{Y_{0it}, i \in \mathcal{C}, t \in \mathcal{T}_0, t \leq T^*\})}_{\text{the posterior density of } \boldsymbol{\theta}_1 \text{ given an external subset } \mathcal{C}} d\boldsymbol{\theta}_1 \right)}_{\text{marginal likelihood}} \times \underbrace{\Pi(\mathcal{C})}_{\text{the prior of } \mathcal{C}}, \end{aligned} \quad (1)$$

where $\pi(\boldsymbol{\theta}_1)$ and $\pi(\boldsymbol{\theta}_1 | \cdot)$ denote the prior and posterior density functions of $\boldsymbol{\theta}_1$, and $L(\{Y_{1it}\}_{t \in \mathcal{T}_1, t \leq T^*} | \boldsymbol{\theta}_1)$ refers to the joint likelihood of the internal data on the time grid

preceding T^* , parameterized by θ_1 . In our application, we designate T^* as 2 years.

We provide further interpretations of (1) to illustrate the rationale behind this selection procedure. On the right-hand side of (1), $\Pi(\mathcal{C})$ denotes our prior guess on external subsets \mathcal{C} 's. In practice, in the absence of this information, we can choose, for example, a uniform prior over all possible \mathcal{C} 's. The remaining term on the right-hand side of (1) is the marginal likelihood (unlike the original definition of the marginal likelihood where the integration is taken over the prior of θ_1 , our definition is more general as it considers the posterior of θ_1 given the external subset \mathcal{C} ; and includes the original definition as a special case if \mathcal{C} is the empty set) that aims to evaluate the similarity between the generating mechanisms of the external subset \mathcal{C} and the internal data, considering data prior to time T^* . In particular, if the selected external subset \mathcal{C} is generated following the same mechanism as the internal data, the marginal likelihood value should be large. On the other hand, if the external subset and internal data follow distinct generating mechanisms, the marginal likelihood should be smaller. Motivated by this property, the posterior distribution in (1) uses the product of the prior and the marginal likelihood to quantify the likeliness that a specific external subset should be selected. We give a theoretical justification in Section 2.2.

Since the marginal likelihood plays an important role in our proposed method, we provide more discussions here. In Bayesian studies, the marginal likelihood is commonly used to quantify the goodness-of-fit for multiple competing models (or priors). The models that assign higher probability masses around the true parameter values (i.e., fit the data better) in general yield higher marginal likelihood values (Robert et al., 2007). One commonly used Bayesian concept derived based on this idea is the Bayes factor. It involves calculating the ratio of the marginal likelihood values between two competitive models M_1 and M_2 . In most cases, a Bayes factor would asymptotically converge to either 0 or $+\infty$ (in probability) as the sample size goes to ∞ , representing M_1 or M_2 is preferred, respectively. In the context of (1), the posterior density functions induced by different subset indexes \mathcal{C}

can be interpreted as the candidate models. During the data selection procedure, the external subset that possesses a higher marginal likelihood can be viewed as having a superior ability to restore the internal data preceding T^* . Note that it is possible that the selection process ends up with selecting all patients in the external dataset. However, instead of naively utilizing all external data, our approach uses a data-driven way to determine which of the external data to incorporate, making it more flexible and robust.

2.2 A theoretical perspective

We first consider a toy example to provide theoretical insights of BASE. Consider the external data $X_1, \dots, X_{N_0} \stackrel{i.i.d.}{\sim} p_{\theta_0}$ and the internal data $Y_1, \dots, Y_{N_1} \stackrel{i.i.d.}{\sim} p_{\theta_1}$, where p_{θ} is a known probability density function with parameter θ . Then we show in the following theorem that by adopting the marginal likelihood in (1) as a criterion for Bayesian estimation with a uniform prior on \mathcal{C} , our method is able to correctly estimate \mathcal{C} as the entire external subset if θ_0 and θ_1 are sufficiently close and the empty set otherwise.

Theorem 2.1. *Suppose $X_1, \dots, X_{N_0} \stackrel{i.i.d.}{\sim} p_{\theta_0}$ and $Y_1, \dots, Y_{N_1} \stackrel{i.i.d.}{\sim} p_{\theta_1}$, and Assumptions (A1)-(A4) detailed in the Supplementary Materials hold. If $\|\theta_0 - \theta_1\|_1 \lesssim \epsilon_{N_0}$, the expected Bayes factor can be controlled as follows,*

$$\frac{\int \prod_{k=1}^{N_1} p_{\theta}(Y_k) d\pi(p_{\theta})}{\int_{\|\theta - \theta_0\|_1 \leq K\epsilon_{N_0}} \prod_{k=1}^{N_1} p_{\theta}(Y_k) d\pi(p_{\theta} \mid \{X_j\}_{j=1}^{N_0})} \xrightarrow{p} 0, \quad \text{as } N_0, N_1 \rightarrow \infty, \quad (2)$$

On the other hand, if $\|\theta_0 - \theta_1\|_1 \gtrsim \epsilon_{N_0} \times \psi_{N_0}$ instead, for ψ_{N_0} diverging to ∞ at any rates, it yields that

$$\frac{\int_{\|\theta - \theta_0\|_1 \leq K\epsilon_{N_0}} \prod_{k=1}^{N_1} p_{\theta}(Y_k) d\pi(p_{\theta} \mid \{X_j\}_{j=1}^{N_0})}{\int \prod_{k=1}^{N_1} p_{\theta}(Y_k) d\pi(p_{\theta})} \xrightarrow{p} 0, \quad \text{as } N_0, N_1 \rightarrow \infty, \quad (3)$$

where $a \lesssim b$ denotes $a \leq C \times b$ for a universal positive constant C , $K > 0$ is defined in the

Supplementary File, $\pi(\cdot)$ is a prior on p_θ , $\epsilon_n = \left(\frac{M_n}{n}\right)^{1/2}$ refers to the posterior contraction rate and $M_n = o(\log n)$ is a sequence of numbers going to ∞ as $n \rightarrow \infty$.

Theorem 2.1 can be viewed as a Bayesian testing (model selection) consistency result. When the external data $\{X_i\}_{i=1}^{N_0}$ is similar to the internal data $\{Y_j\}_{j=1}^{N_1}$, i.e., θ_0 and θ_1 are sufficiently close, the marginal likelihood of the internal data, obtained by integrating over the posterior density given the external data, dominates the likelihood integrated over the prior. In other words, the external data provides additional useful information in this case compared to using internal data only and the magnitude of marginal likelihood is able to reflect that. Contrarily, when the external and internal data sets are significantly distinct, the marginal likelihood merely given by the prior will be preferred, i.e., the marginal likelihood only selects the internal data to use.

Assumptions (A1)-(A4) in Theorem 2.1 can be interpreted as follows: (A1) The model parameter θ is finite-dimensional and the prior distribution of θ has a large support; (A2) Both θ_0 and θ_1 can be consistently estimated based on the external data $\{X_j\}_{j=1}^{N_0}$ and the internal data $\{Y_k\}_{k=1}^{N_1}$; (A3) The external data size N_0 is smaller than the internal data size N_1 at a specific rate; and (A4) The Kullback-Leibler neighbors include the ℓ_1 neighbors, for θ_0 and θ_1 . Assumption (A1) is easily satisfied since p_θ is a parametric model. Assumptions (A2) and (A4) are testable and widely used in Bayesian asymptotics literature; and they can be easily verified following the steps of Lemma 8.1 and Theorem 2.1 in Ghosal et al. (2000) and Lemma B2 in Shen et al. (2013). Assumption (A3) requires the internal data size to be larger than the external data size, which is reasonable given that we would like to only borrow information from the external set while treating the internal data as the main source for inference.

Next we consider a more realistic scenario where the internal data Z_1, \dots, Z_{N_1} is still generated from p_{θ_0} , but the external data consist of $X_1, \dots, X_{N_0^*} \stackrel{i.i.d.}{\sim} p_{\theta_0}$ and $Y_1, \dots, Y_{N_0'} \stackrel{i.i.d.}{\sim} p_{\theta_1}$. In the next theorem, we show that our method is capable of identifying the correct

external subset $\{X_i\}_{i=1}^{N_0^*}$, with a cost of at most including a small amount of data from the incorrect external subset $\{Y_j\}_{j=1}^{N_0'}$. The key observation is that if a non-ignorable proportion of $\{Y_j\}_{j=1}^{N_0'}$ is included, the induced density function, a mixture of p_{θ_0} and p_{θ_1} , diverges from p_{θ_0} at a recognizable distance, hence will be detected by our method. Theorem 2.2 holds under Assumption (A1), (A3), (B1), (C1) and (C2). Briefly speaking, (B1) and (C2) are the modifications of (A2) and (A4) given pooled samples; (C1) assumes that N_0^* tends to ∞ as $N_0 \equiv N_0^* + N_0'$ approaches ∞ .

Theorem 2.2. *Suppose Assumptions (A1), (A3), (B1), (C1) and (C2) in the Supplementary File hold. Let $m' \leq N_0'$ be the number of subjects selected from the incorrect subset $\{Y_j\}_{j=1}^{N_0'}$. If m' satisfies $\|p_{\theta_0} - p_{\theta_1}\|_1 = o\left(\frac{m'+N_0^*}{m'} \times \left(\sqrt{\frac{M_{m'+N_0^*}}{m'+N_0^*}} - \sqrt{\frac{M_{N_1}}{N_1}}\right)\right)$, we have*

$$\frac{\int_{\|p_{\theta} - p_{u,v}^*\|_1 \leq K^* \epsilon_{u+v}} \prod_{k=1}^{N_1} p_{\theta}(Z_k) d\pi(p_{\theta} \mid \{X_i\}_{i=1}^u, \{Y_j\}_{j=1}^v)}{\int_{\|p_{\theta} - p_{N_0^*, m'}^*\|_1 \leq K^* \epsilon_{N_0^* + m'}} \prod_{k=1}^{N_1} p_{\theta}(Z_k) d\pi(p_{\theta} \mid \{X_i\}_{i=1}^{N_0^*}, \{Y_j\}_{j=1}^{m'})} \xrightarrow{p} 0, \quad \text{as } N_0^*, N_0, u, v \rightarrow \infty \quad (4)$$

if either of the following two conditions holds (i) $\frac{u+v}{v} \times \left(\sqrt{\frac{M_{N_1}}{N_1}} + \sqrt{\frac{M_{u+v}}{u+v}}\right) = o(\|p_{\theta_0} - p_{\theta_1}\|_1)$ or (ii) $u + v = o(N_0^* + m')$, where $M_n = o(\log n)$ is a sequence of numbers going to ∞ as $n \rightarrow \infty$, $\epsilon_n = \left(\frac{M_n}{n}\right)^{1/2}$, u and v denote the number of subjects selected from the correct and incorrect external subsets, respectively, $p_{n,m}^* \equiv \frac{n}{n+m}p_{\theta_0} + \frac{m}{n+m}p_{\theta_1}$ refers to the weighted average of p_{θ_0} and p_{θ_1} given $n \leq N_0^*$, $m \leq N_0'$, and $n, m \in \mathbb{Z}^+$.

Theorem 2.2 states that our model (induced by the posterior $\pi(\cdot \mid \{X_i\}_{i=1}^{N_0^*}, \{Y_j\}_{j=1}^{m'})$) that selects the entire correct external subset $\{X_i\}_{i=1}^{N_0^*}$ plus m' subjects from the incorrect subset $\{Y_j\}_{j=1}^{N_0'}$ is preferred over alternative models $\pi(\cdot \mid \{X_i\}_{i=1}^u, \{Y_j\}_{j=1}^v)$ in terms of the marginal likelihood values. The proportion of incorrect selection $\frac{m'}{N_0^*}$ is decided by the discrepancy between p_{θ_0} and p_{θ_1} . For example, if the discrepancy is small, e.g., 0, then m' can be as large as N_0^* because there is no incorrect subset. When the discrepancy is large,

then m' becomes negligible compared to N_0^* . The number of subjects u and v are assumed to satisfy (i) $p_{u,v}^* \equiv \frac{u}{u+v}p_{\theta_0} + \frac{v}{u+v}p_{\theta_1}$ is recognizably distant from p_{θ_0} , or (ii) $\{X_i\}_{i=1}^u, \{Y_j\}_{j=1}^v$ is not as informative as $\{X_i\}_{i=1}^{N_0^*}, \{Y_j\}_{j=1}^{m'}$. Notably, when $u+v$ is finite, the result still holds by slightly modifying the proof of Theorem 2.1.

Theorem 2.1 and 2.2 justify the data selection procedure with the marginal likelihood criteria. Specifically, the model can select the correct external subset $\{X_i\}_{i=1}^{N_0^*}$ at an order of $O(N_0^*)$, while discarding the wrong external subset $\{Y_j\}_{j=1}^{N_0'}$ except for a negligible proportion. Motivated by these theoretical results under i.i.d. assumptions, our selection criterion (1) uses the first half (preceding T^*) of the follow-up studies to explore the relevant external subset. This reduces bias in estimating the early-stage parameters, compared to directly combining the internal and external data. Moreover, introducing the external trajectories is beneficial for revealing the long-term efficacy. The validity and performance of this procedure will be further studied in Section 4 through numerous simulations.

3 Model specification for the hemophilia study

3.1 Concatenated Cubic Hermite spline

In this section, we introduce a parametric model to characterize the trend of factor level. Motivated by a shared pattern among similar gene therapy products, i.e., factor level that increases after the treatment may decrease over time and eventually reach a plateau value (Nathwani et al., 2018; Shah et al., 2023), we propose to model the outcome mean trend using a concatenation of two Cubic Hermite splines. Specifically, for trajectory i in study s , we model the outcome mean trend using $\psi(t; \boldsymbol{\theta}_{si})$, for $t \in [0, T]$, parametrized by $\boldsymbol{\theta}_{si} \equiv (\mu_{s0i}, m_{s0i}, \mu_{s1i}, m_{s1i}, \mu_{s2i})$, which is defined using two Cubic Hermite splines, over

two intervals $[0, \alpha]$ and $(\alpha, T]$ and concatenated at a turning point α , i.e.,

$$\psi(t; \boldsymbol{\theta}_{si}) = \begin{cases} h_{00}(\frac{t}{\alpha})\mu_{s0i} + h_{10}(\frac{t}{\alpha})\alpha m_{s0i} + h_{01}(\frac{t}{\alpha})\mu_{s1i} + h_{11}(\frac{t}{\alpha})\alpha m_{s1i}, & t \in [0, \alpha], \\ h_{00}(\frac{t-\alpha}{T-\alpha})\mu_{s1i} + h_{10}(\frac{t-\alpha}{T-\alpha})(T-\alpha)m_{s1i} + h_{01}(\frac{t-\alpha}{T-\alpha})\mu_{s2i}, & t \in (\alpha, T], \end{cases} \quad (5)$$

where T is a pre-specified time point at which the outcome has reached a plateau (in our application, T represents five years). For trajectory i in study s , μ_{s0i} and m_{s0i} represent the starting value and the corresponding derivative at $t = 0$, respectively, μ_{s1i} and m_{s1i} respectively denote the factor level value and the corresponding derivative at the turning point α , and μ_{s2i} represents the final value at the plateau point $t = T$, where the derivative is 0. In addition, $h_{00}, h_{10}, h_{01}, h_{11}$ are the Cubic Hermite basis functions, defined as $h_{00}(t) = 2t^3 - 3t^2 + 1$, $h_{10}(t) = t^3 - 2t^2 + t$, $h_{01}(t) = -2t^3 + 3t^2$, and $h_{11}(t) = t^3 - t^2$. In Figure 2, we illustrate a mean function $\psi(t; \boldsymbol{\theta}_s)$ with the parameters annotated.

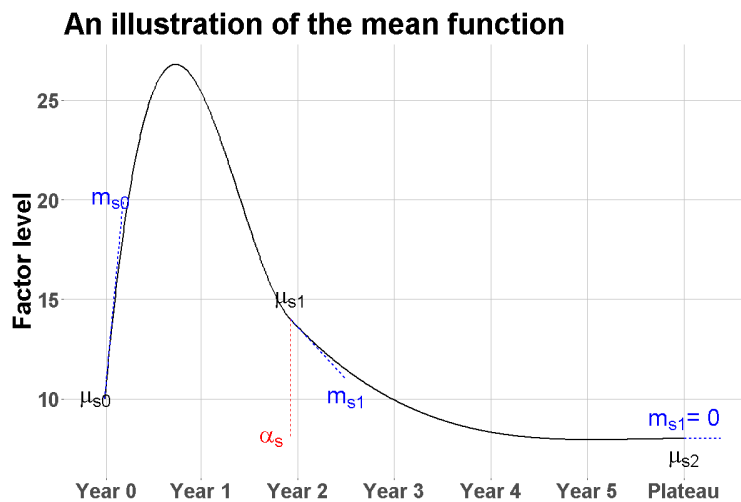


Figure 2: The blue dashed lines represent the derivatives at specific time points, while the black solid line illustrates the mean value. The turning point is indicated by the red dashed line.

Our choice of using a concatenated Cubic Hermite spline has three-fold benefits. First, it facilitates incorporating the trend information, e.g., the factor level that increases after the treatment may decrease over time, as suggested by [Nathwani et al. \(2018\)](#). For instance,

consider a population-level trend for study s , namely,

$$\boldsymbol{\theta}_s \equiv (\mu_{s0}, m_{s0}, \mu_{s1}, m_{s1}, \mu_{s2}) = \sum_{i=1}^{n_s} \frac{1}{n_s} (\mu_{s0i}, m_{s0i}, \mu_{s1i}, m_{s1i}, \mu_{s2i}),$$

where n_s represents the number of trajectories in study s . If we impose a constraint that m_{s0} is positive and m_{s1} is negative, the concatenated Cubic Hermite spline is able to mimic the initially increasing and subsequently decreasing trend. Second, the parameterization motivates a strategy for selecting the relevant external data, i.e., the $\boldsymbol{\theta}_s$ estimated based on the selected external data should be close to the one given by the internal data. This provides empirical evidence to explore external subsets perceived as similar to the internal data preceding T^* . Here we assume the existence of external subsets with a $\boldsymbol{\theta}_s$ similar to the one from the internal data. In Section 4, we explore the situations when this assumption is violated. Third, the concatenated Cubic Hermite spline can be expressed as a linear span of the basis functions of a Cubic Hermite spline, piece-wisely within each of the two time intervals segmented at α . From a Bayesian computation perspective, this property allows us to adopt a multivariate normal prior on $\boldsymbol{\theta}_s$ for conjugacy and computational efficiency.

In the following section, we will outline the procedure for selecting the relevant external data based on this parameterization. It is important to note that adopting the concatenated Cubic Hermite spline to model the underlying trend might introduce a potential risk of underfitting in practice due to its parametric nature. However, the advantage lies in the efficient posterior sampling. Moreover, considering the limited nature of the external data in the collected hemophilia dataset, opting for a more complex model could result in unstable inferences regarding our primary research interests, such as the plateau value. Therefore, we choose concatenated Cubic Hermite splines to trade mild underfitting for a substantial increase in modeling efficiency and robustness.

3.2 Full model specification

We present our model before applying the data selection strategy in Section 2. The proposed model can be outlined in the following hierarchical order.

$$\begin{aligned}
Y_{1it} &= \psi(t; \boldsymbol{\theta}_{1i}) + \epsilon_{1it}, \text{ for } i = 1, \dots, N_1, \quad Y_{0jt} = \psi(t; \boldsymbol{\theta}_{0j}) + \epsilon_{0jt}, \text{ for } j \in \mathcal{C}, \\
\psi(t; \boldsymbol{\theta}_{si}) &= \begin{cases} h_{00}(\frac{t}{\alpha})\mu_{s0i} + h_{10}(\frac{t}{\alpha})\alpha m_{s0i} + h_{01}(\frac{t}{\alpha})\mu_{s1i} + h_{11}(\frac{t}{\alpha})\alpha m_{s1i}, & t \in [0, \alpha] \text{ and } t \in \mathcal{T}_s, \\ h_{00}(\frac{t-\alpha}{T-\alpha})\mu_{s1i} + h_{10}(\frac{t-\alpha}{T-\alpha})(T-\alpha)m_{s1i} + h_{01}(\frac{t-\alpha}{T-\alpha})\mu_{s2i}, & t \in (\alpha, T] \text{ and } t \in \mathcal{T}_s, \end{cases} \\
\boldsymbol{\theta}_{1i}, \boldsymbol{\theta}_{0j} &\stackrel{i.i.d.}{\sim} N(\beta^*, \Sigma^*), \text{ for } i = 1, \dots, N_1, \quad j \in \mathcal{C}, \text{ with} \\
\boldsymbol{\theta}_{si} &\equiv (\mu_{s0i}, m_{s0i}, \mu_{s1i}, m_{s1i}, \mu_{s2i})^T, \text{ for } s = 0, 1, \\
\beta^* | \Sigma^* &\sim N^{(2^+, 4^-)}(\beta_0, \Sigma^*), \\
\Sigma^{*-1} &\sim W(\nu_0, \Psi_0), \\
(\epsilon_{sit})_{t \in \mathcal{T}_s} | \sigma_s^2, \rho &\sim N(0, \sigma_s^2 \times \Sigma_\rho), \quad \sigma_s^{-2} \sim \text{Gamma}(a_0, b_0), \\
\alpha &\sim tN(\text{mean} = 2, \text{sd} = 1; \text{lb} = 0, \text{ub} = T), \quad \rho \sim \text{Unif}(0, 1), \\
\mathcal{C} &\sim \Pi(\mathcal{C} | \{Y_{sit}, i = 1, \dots, N_s, t \in \mathcal{T}_s, t \leq T^*, s = 0, 1\}),
\end{aligned} \tag{6}$$

where θ_{1i} and θ_{0j} refer to the individual-wise parameter of the concatenated Cubic Hermite spline for both external and internal data, respectively. Here, α is common for $s = 0$ and $s = 1$ to increase the external information borrowing ratio, $N^{(2^+, 4^-)}$ refers to a multivariate normal distribution that is truncated above 0 for the second entry and below 0 for the fourth entry, as discussed in Section 3.1, Σ_ρ denotes a covariance matrix with the auto-regressive structure, with the (k, l) entry being $\rho^{|k-l|}$ for any $k, l \in \mathcal{T}_s$, and $tN(\text{mean} = 2, \text{sd} = 1; \text{lb} = 0, \text{ub} = T)$ refers to a normal distribution $N(2, 1)$ truncated between 0 and T . The hyperparameters such as the mean and the standard deviation are derived from previous studies, i.e., [Samelson-Jones et al. \(2021\)](#), available in Section 5 of the Supplementary File.

This suggests that the turning point is likely to occur around the second year since the treatment, with a one-year standard deviation as uncertainty. The posterior distribution of \mathcal{C} shown in the last display of (6) is defined as follows,

$$\begin{aligned} & \Pi(\mathcal{C} \mid \{Y_{sit}, i = 1, \dots, N_s, t \in \mathcal{T}_s, t \leq T^*, s = 0, 1\}) \\ & \propto \int \prod_{i=1}^{N_1} \prod_{t \in \mathcal{T}_1, t \leq T^*} L(Y_{1it} \mid \beta^*, \Sigma^*, \alpha, \rho, \sigma_0^2, \sigma_1^2) \times \\ & \quad \pi(\beta^*, \Sigma^*, \alpha, \rho, \sigma_0^2, \sigma_1^2 \mid \{Y_{0it}, i \in \mathcal{C}, t \in \mathcal{T}_0, t \leq T^*\}) d\beta^* d\Sigma^* d\alpha d\rho d\sigma_0^2 d\sigma_1^2, \end{aligned} \quad (7)$$

where $L(\cdot \mid \beta^*, \Sigma^*, \alpha, \rho, \sigma_0^2, \sigma_1^2)$ denotes the likelihood function by marginalizing out the individual-wise trend information, and $\pi(\beta^*, \Sigma^*, \alpha, \rho, \sigma_0^2, \sigma_1^2 \mid \{Y_{0it}, i \in \mathcal{C}, t \in \mathcal{T}_0, t \leq T^*\})$ refers to the posterior density function given the first half of the follow-up data.

Model (6) needs more interpretations for clarification. To account for the high within-study variation observed in Figure 1(a), we consider a mixed-effects model structure instead of solely relying on the Gaussian error term ϵ_{sit} to absorb the variation. This is inspired by the observation from Figure 1(a) that the internal (phases 2b and 3) trajectories appear to have an increasing variation level progressively, which is hardly modeled either by using a large σ_s^2 or imposing commonly-used temporal structures. In addition, it is crucial to highlight that the variables Y_{1it} and Y_{0it} in (6) have been z-transformed following the steps specified in Section 1.3. The z-transformation, to some extent, forces the starting value and the corresponding variance across the studies to be the same, i.e., the first entry of β^* to be 0 and the first diagonal term of Σ^* to be 1 for both the studies. This normalization potentially increases the proportion of external data that can be borrowed by the internal data based on Model (6).

For both simulation and real data analysis, we consider the following hyper-parameter settings for the priors, $\beta_0 = (0, 0, 0, 0, 0)^T$, $\nu_0 = 0.01$, $\Psi_0 = 100 \times \text{diag}(1, 1, 1, 1, 1)$, $a_0 = 0.01$, $b_0 = 0.01$ and $\Pi(\mathcal{C}) \propto 1$. Besides, for the real data analysis, we choose $T^* = 2$ and $T = 6$,

which refer to the latest endpoint of the 2.5-year follow-up study and assume the factor level will approach the plateau value at the sixth year after the treatment. The simulation settings will be given in Section 4. We will conduct sensitivity analyses to study whether it significantly changes the inference result by increasing T . For the sampling procedure, we consider 1,000 MCMC iterations, with the first half being the burn-in samples. Empirically, the chosen priors are sufficiently non-informative, and the iteration number is enough to approach the stationary posterior distribution with a well-mixing. Additionally, the most time-consuming task, when deployed on a server that operates at 3.80 GHz, takes approximately 16 hours. This duration is considered bearable for a Bayesian method. The efficiency of the task is attributed to the conjugacy achieved by adopting the multivariate-normal inverse-Wishart distribution and inverse-Gamma distribution, as defined in (6). In Section 4, we will further investigate the performance of our proposed model.

4 Simulation

We conduct simulations to evaluate the performance of our method. Throughout, we generate the internal data as follows: 40 trajectories are generated given $\beta^* = (20, 1, 10, -0.1, 8)$, $\Sigma^* = \text{diag}(25, 0.1, 9, 0.1, 4)$, $\alpha = 2.5$, $T = 5$ and $\rho \in \{0, 0.5\}$. The number of observations for each trajectory n_i follows $\text{Pois}(20)$ with the time grids $t_1, \dots, t_{n_i} \stackrel{i.i.d.}{\sim} \text{Unif}(0, 2.5)$.

We consider four data-generating processes (DGPs) for generating K trajectories in the external study: (DGP 1) $\beta^* = (20, 1, 10, -0.1, 8)$; (DGP 2) $\beta^* = (20, 1, 10, -0.1, 12)$; (DGP 3) the first $K/2$ trajectories from $(20, 1, 10, -0.1, 8)$ and the second $K/2$ trajectories from $\beta^* = (10, 4, 20, -1, 8)$; (DGP 4) the first $K/2$ trajectories from $(20, 1, 10, -0.1, 8)$ and the second $K/2$ trajectories from $(10, 4, 20, -1, 12)$.

In DGP 1 and DGP 2, we investigate the ability of our model to borrow long-term information from the external data. We generate the external data using the same process

as the internal data before a specific time point, i.e., $(\mu_{s0}, m_{s0}, \mu_{s1}, m_{s1})$ are the same for $s = 0, 1$. This allows us to assess whether the internal data can benefit from the external subset selection in achieving a precise plateau value estimate. Furthermore, we let the plateau value be the same (DGP 1) or different (DGP 2) across the two studies to examine the robustness of the plateau value estimated through the selection procedure. The overall θ_s is different across the external and internal data for DGP2 due to different μ_{s2} values. In summary, DGP 1 is to examine our method under the true model, and DGP 2 aims to check the μ_{s2} estimation when $\mu'_{s2}s$ are distinct.

In DGP 3 and DGP 4, we consider a mix of trajectories from the external data, half following the same data-generating process as the internal data and the other half do not, i.e., $m' = N'_0/2$ preceding T^* . The main purpose is to examine whether our method has the ability to select the correct subset, as well as the efficiency of information borrowing when the external data are significantly distinct from the internal data. We let the plateau value be the same (DGP 3) or different (DGP 4) across the two studies. For DGP3, we let μ_{s2} stay the same regardless of the θ'_s values, and for DGP4 only allow subjects with the correct θ'_s to have the same μ_{s2} with the one in the internal data design. The rest of the parameters are set the same for all DGPs: $\Sigma^* = \text{diag}(25, 0.1, 9, 0.1, 4)$, $\alpha = 2.5$, $K \in \{20, 40\}$, $T = 5$ and $\rho \in \{0, 0.5\}$. The number of observations for each trajectory n_i follows $\text{Pois}(20)$ with the time grid $t_1, \dots, t_{n_i} \stackrel{\text{i.i.d.}}{\sim} \text{Unif}(0, 5)$.

To emulate the observation from the real data that the internal data are censored after the 2.5-year time point, we terminate the collection of the internal data by generating the time grid for each observation from $\text{Unif}(0, 2.5)$, while the total follow-up duration is $T = 5$. The upper bound of 2.5 is intentionally set to be the same with α such that the estimation of the fifth entry of β^* , the plateau value (beyond α), becomes challenging due to the lack of data without the incorporation of external data. In Figure 3, we generate one simulated data for each scenario. DGP 1 and 2 assume the same distribution between external and

internal data before 2.5 years, while DGP 3 and 4 do not. DGP 1 and 3 use the same plateau values between external and interval data, while DGP 2 and 4 do not.

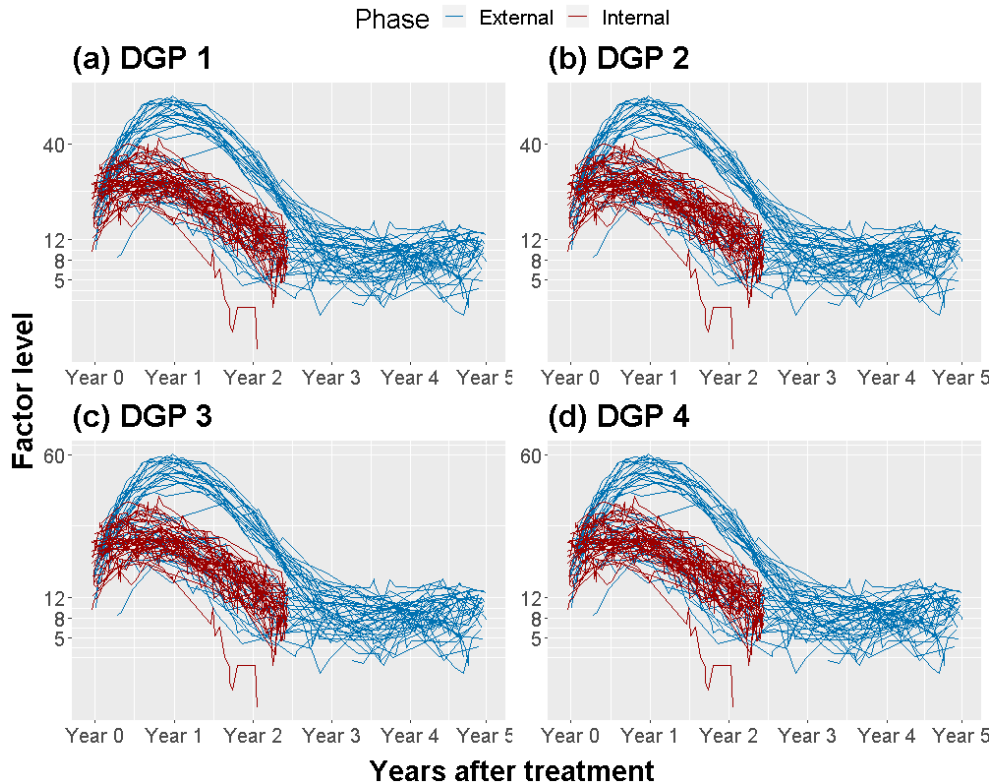


Figure 3: Simulated sample data under each data generation process (DGP).

We assess the performance of our method using two metrics: the relative error and the external proportion selected during the posterior sampling. The relative error is utilized to measure the accuracy of both the starting value and the plateau value estimation. We use ℓ_{Start} and ℓ_{Plateau} to denote them, respectively, and define them as follows,

$$\begin{aligned} \ell_{\text{Start}} &= \text{median} \left\{ \sum_{k=1}^2 \left| \frac{\hat{\beta}_{k,l} - \beta_k^*}{\beta_k^*} \right| \right\}_{l=1}^M, \\ \ell_{\text{Plateau}} &= \text{median} \left\{ \left| \frac{\hat{\beta}_{5,l} - \beta_5^*}{\beta_5^*} \right| \right\}_{l=1}^M, \end{aligned} \tag{8}$$

where M is the number of posterior samples remaining after burn-in, β_j^* denotes the j -th entry of β^* and $\hat{\beta}_{j,l}$ is the corresponding posterior sample obtained at the l -th iteration after

the burn-in. To evaluate the efficiency of information borrowing, we examine the external proportion, denoted by,

$$p_{Ext} = \text{median} \left\{ \frac{|\mathcal{C}_l|}{K} \right\}_{l=1}^M, \quad (9)$$

where $|\mathcal{C}_l|$ is the size of the external subset (number of trajectories) selected at the l -th iteration after the burn-in, and K refers to the size of the entire external data (total trajectories). Our method is compared with the direct combination of the internal and external data under ℓ_{Start} and ℓ_{Plateau} , while p_{Ext} is only considered for our model.

We also compare the metrics ℓ_{Start} and ℓ_{Plateau} for both methods using p_{ifSmall} and p_{sPlateau} , which counts the proportion of times when our method (BASE) achieves a smaller value in ℓ_{Start} and ℓ_{Plateau} , respectively than the direct combination based on the posterior samples. Similarly, we let p_{ifPrefer} denote the frequency that the correct half of the external data is favored for DGP 3 and 4, i.e., the number of selected trajectories for the correct half is no less than that for the wrong half. The results are presented in Table 1 and 2.

We first discuss Table 1. When data preceding T^* are generated under the true model (DGP 1 and 2), both methods achieve comparable accuracy in estimating the starting parameters, indicated by the close ℓ_{Start} values, which is of our expectation. On the other hand, when data are generated incorrectly (DGP 3 and 4), the data selection procedure demonstrates a remarkable reduction in ℓ_{Start} compared to the direct combination method. This observation is also supported by the p_{ifSmall} columns in Table 2, i.e., $p_{\text{ifSmall}} \geq 89\%$ for DGP 3 and 4. For the plateau value estimation, our method also achieves a more accurate estimation than direct combination, as evident from the observation that the p_{sPlateau} values are consistently above 60% in Table 2. This advantage becomes particularly pronounced under DGP 4, where a subset of the external data is generated differently from the internal data, our method achieves significantly lower values in ℓ_{Start} and ℓ_{Plateau} , along with high

Table 1: Median (The interquartile range; Q3 - Q1) of the three statistics over 100 Monte Carlo replications for each of the four DGPs given different sample sizes K .

			Data selection (BASE)			Direct combination	
K	ρ	DGP	ℓ_{Start}	ℓ_{Plateau}	p_{Ext}	ℓ_{Start}	ℓ_{Plateau}
20	0.0	1	0.11 (0.04)	0.18 (0.17)	0.85 (0.11)	0.11 (0.05)	0.20 (0.21)
	0.5		0.12 (0.04)	0.18 (0.17)	0.70 (0.15)	0.12 (0.06)	0.21 (0.22)
40	0.0		0.10 (0.04)	0.21 (0.26)	0.85 (0.10)	0.10 (0.06)	0.22 (0.30)
	0.5		0.11 (0.05)	0.20 (0.23)	0.69 (0.18)	0.11 (0.06)	0.22 (0.31)
20	0.0	2	0.12 (0.04)	0.37 (0.36)	0.85 (0.11)	0.11 (0.05)	0.38 (0.39)
	0.5		0.12 (0.04)	0.35 (0.25)	0.70 (0.20)	0.12 (0.06)	0.40 (0.35)
40	0.0		0.10 (0.05)	0.44 (0.42)	0.84 (0.08)	0.10 (0.05)	0.45 (0.42)
	0.5		0.11 (0.04)	0.43 (0.41)	0.70 (0.15)	0.11 (0.06)	0.45 (0.44)
20	0.0	3	0.20 (0.11)	0.21 (0.21)	0.80 (0.15)	0.24 (0.16)	0.22 (0.28)
	0.5		0.17 (0.09)	0.23 (0.21)	0.60 (0.15)	0.25 (0.16)	0.22 (0.28)
40	0.0		0.24 (0.16)	0.24 (0.22)	0.73 (0.30)	0.33 (0.18)	0.23 (0.26)
	0.5		0.23 (0.11)	0.23 (0.19)	0.60 (0.15)	0.33 (0.17)	0.25 (0.26)
20	0.0	4	0.20 (0.11)	0.22 (0.23)	0.80 (0.15)	0.30 (0.18)	0.43 (0.25)
	0.5		0.17 (0.08)	0.24 (0.20)	0.60 (0.11)	0.30 (0.17)	0.43 (0.25)
40	0.0		0.25 (0.15)	0.26 (0.26)	0.73 (0.25)	0.40 (0.15)	0.54 (0.20)
	0.5		0.22 (0.09)	0.26 (0.24)	0.60 (0.13)	0.40 (0.16)	0.53 (0.21)

values in p_{ifPrefer} and p_{sPlateau} . This underscores that our method effectively selects the correct subset from the external data with high probabilities.

We have conducted additional simulation studies to assess the sensitivity of our method by varying hyperparameter values and plateau points. Moreover, we explored the impact of generating random errors from heavy-tailed t-distributions instead of the normal distribution in our model. The results are summarized in Section 3 and 4 of the Supplementary File, and they are consistent with the findings in Table 1 and 2. All these findings confirm the robustness of our method and its effectiveness in terms of selecting the correct subset from external data and reducing estimation bias in parameter estimation.

Table 2: The three frequency values that compare the data selection procedure to the direct combination.

K	ρ	DGP	p_{ifSmall}	p_{sPlateau}	DGP	p_{ifSmall}	p_{ifPrefer}	p_{sPlateau}
20	0.0	1	0.44	0.63	3	0.89	0.74	0.44
	0.5		0.39	0.61		0.90	0.97	0.5
40	0.0		0.44	0.73		0.97	0.74	0.62
	0.5		0.39	0.74		1.00	0.90	0.67
20	0.0	2	0.49	0.62	4	0.96	0.71	0.91
	0.5		0.42	0.65		0.93	0.97	0.82
40	0.0		0.45	0.66		0.99	0.74	0.97
	0.5		0.39	0.64		1.00	0.86	0.97

5 Long-term outcome after a hemophilia gene therapy

5.1 Data description and clinical question of interest

The data were collected from three studies of different phases designed to assess the effectiveness of gene therapy as a long-term therapeutic solution for hemophilia B. The study focuses on monitoring the factor IX (FIX) activity levels of the subjects after receiving treatment with a therapy involving an adeno associated virus 5 (AAV5) vector. In this work, we treat the 10 trajectories from the phase 1 study, with a 5-year follow-up, as the external data. The 3 trajectories from the phase 2b study and the 54 trajectories from the phase 3 study are considered as the internal data, with both studies having a follow-up period of up to 2.5 years. The clinical question of interest is to make annual predictions on the FIX activity level and provide statistical evidence to validate whether the FIX activity level increases at the end of the fifth year compared with the initial level, based on the prediction.

We provide a brief overview of the design and objectives of the three study phases, with more detailed information available in the cited references for interested readers. Phase 1 study (NCT02396342; [Miesbach et al. \(2021\)](#)) focused on assessing the safety and efficacy of AMT-060 gene therapy and involved 10 male participants with severe or moderate-

severe hemophilia B. Phase 2b study (NCT03489291; [Gomez et al. \(2021\)](#)) was an open-label, single-dose, single-arm, multi-center trial, and it involved 3 adult participants with severe hemophilia B. The main goal was to assess the sustained efficacy of HEMGENIX (also called by AMT-061), which is the first FDA approved gene therapy for hemophilia B. Phase 3 study (NCT03569891; [Pipe et al. \(2023\)](#)) enrolled 54 men with moderate-to-severe hemophilia B to evaluate the change in the annualized bleeding rate post-treatment compared to the rate during the lead-in period. The participants received a single infusion of HEMGENIX. Detailed demographic and clinical characteristics of the participants in Phase 3 study can be found in [Pipe et al. \(2023\)](#) and Table 1 therein.

5.2 Primary analysis

We implement our data selection method to analyze the Hemophilia data. For the posterior sampling, we use the same hyperparameter settings as those introduced in Section 3.2 and consider 1,000 MCMC iterations, with the first 500 iterations discarded as the burn-in samples. To obtain a representative result, we conducted our selection procedure 100 times and studied the variation of the posterior median for both the starting value and the plateau value. The result indicates that the median values for the starting value and the plateau value are 26.86 (with a standard deviation of 0.09) and 32.08 (with a standard deviation of 0.21), respectively, over the 100 replications. These findings further indicate that it is trustworthy to study a single chain because the across-chain variation is tolerable. Based on one of the 100 chains, we visualize the estimated trend in the top panel of Figure 4 using the posterior median of β^* , with a 95% credible region banded by the 2.5% and 97.5% quantiles of the posterior samples. In particular, we mark out the 95% credible interval for each of the five years aligned with the estimated trend.

According to the posterior samples of the chain presented, the median values of the predicted starting and plateau values are 26.93 (with a 95% credible interval of [23.21, 30.11])

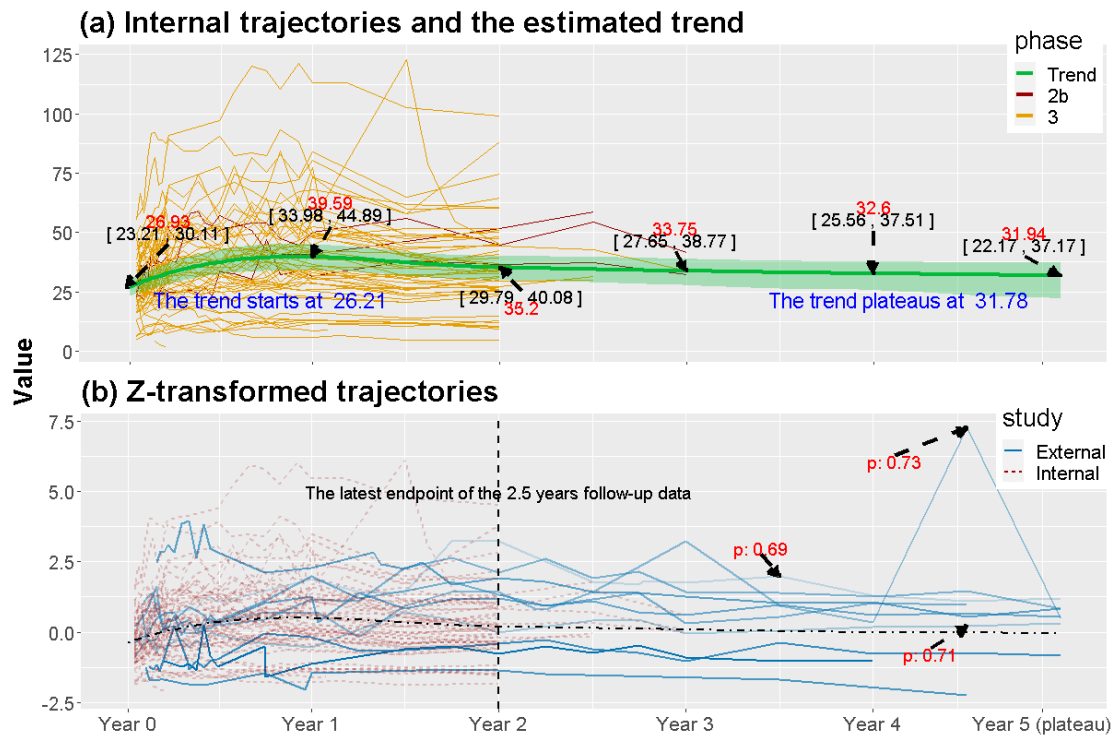


Figure 4: (a) The spaghetti plot of the internal trajectories and the trend estimated based on the BASE. The green banded region refers to the 95% credible interval; (b) The external trajectories presented with their opacity proportional to the corresponding posterior frequency of being selected. The dot-dashed line refers to the estimated trend.

and 31.94 (with a 95% credible interval of [22.17, 37.17]), respectively. Despite being fitted using internal data up to 2.5 years, our model yields a 95% credible interval at Year 3 of [27.65, 38.77], which contains the actual median FIX activity level (36.0) reported in the Phase 3 study (available at <https://ash.confex.com/ash/2023/webprogram/Paper187624.html>). This strongly validates our proposed method. To answer the scientific question of whether there is statistically significant evidence to assert that the predicted plateau value is greater than the starting value, we further examine the posterior probability that the predicted plateau value exceeds the predicted starting value. Based on the posterior samples, the estimated probability is 93%, which strongly supports our hypothesis. Another finding is that the bandwidth of the credible interval increases annually with the trend over the five years, as shown in Figure 4(a). This finding is partly attributed to the reduction in the effective sample size informing the trend as it progresses, primarily due to the internal

data being censored after the 2.5-year follow-up endpoint.

We also investigate to which extent each external trajectory is preferred by the internal dataset, quantified by the posterior probability of selection. These results are presented in Figure 4(b) using opacity, where lighter colors indicate smaller probabilities, representing the degree to which each external trajectory is preferred. We highlight three trajectories that are least preferred as they have the lowest posterior probabilities of being selected (e.g., 0.69, 0.71, and 0.73). In addition, the posterior median of the selected external proportion is 0.80, with a standard deviation of 0.25. This result suggests that the majority of the external trajectories can be utilized based on the internal information, implying a significant similarity between the internal and external data after applying Z-transformation. From a scientific perspective, the high proportion of external data utilization may indicate that the mechanism of action of hemophilia and durability of gene therapy remains consistent between AMT-060 (external data) and etranacogene dezaparvovec, which differ by 1 single amino acid resulting in naturally occurring highly active FIX Padua variant (FIX-R338L). Furthermore, it supports the hypothesis that this evolution only influence the baseline and plateau factor levels after the subjects are treated. Moreover, by examining the study subjects that are frequently selected, one could identify potential external sub-populations exhibiting the same trend as the internal population before the follow-up endpoint. Such insights could be valuable for future research endeavors.

5.3 Secondary analysis

We conduct a two-fold secondary analysis. First, we compare the results given by our proposed method (Selection) with those from the direct combination (Combination) and no-information-borrowing (No-borrow) from the external dataset. Second, we evaluate the robustness of our model by considering different prior hyper-parameter settings.

We present the estimated trends along with their credible intervals obtained by the

three methods under the same MCMC settings in Figure 5(a) and (b). Additionally, we display the estimated annual factor levels and the turning point in Table 3. All three methods yield similar results in the early stage, specifically before Year 2, which is due to the availability and dominance of the internal trajectories before 2.5 years. The curve obtained without using external information (No-borrow) exhibits high variance starting from the middle period of the 5-year duration due to the absence of long-term data. This is also reflected by the large standard deviations in the estimated factor levels at the fourth and fifth years in Table 3. Both our method and the direct combination method yield similar estimated trends and plateau values. This similarity arises because our method selects a high proportion (around 80%) of the external data for inference. However, our method achieves this estimate in a more robust and principled way.

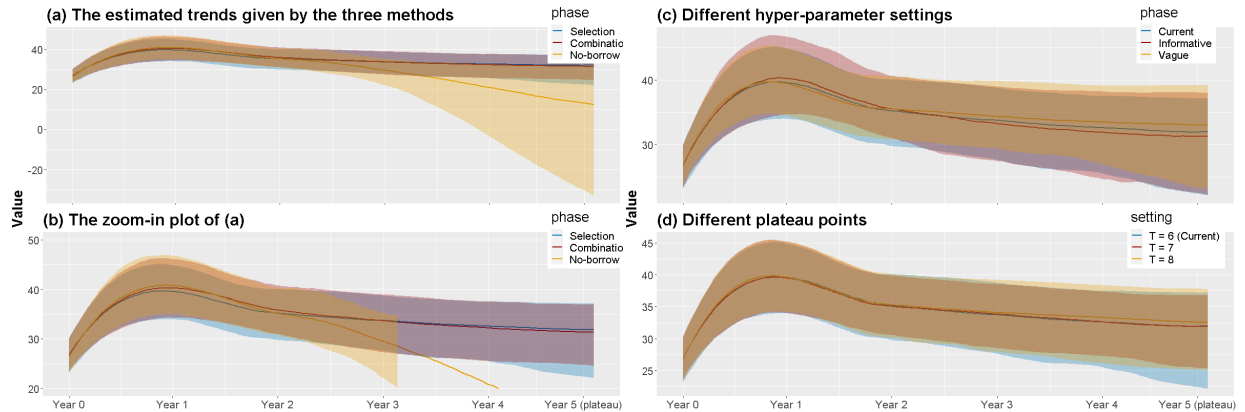


Figure 5: (a) The estimated trends (median) together with their 95% credible intervals obtained by the three methods; (b) The zoom-in plot of (a); (c) The sensitivity analysis results under different hyper-parameter settings; (d) The sensitivity analysis results with different plateau time points.

To investigate the robustness of our results, we perform a sensitivity analysis by adopting alternative prior hyperparameter values ν_0, Ψ_0, a_0, b_0 defined in (6) and plateau time points T . Specifically, we consider a more informative prior (Informative) and a vaguer prior (Vague) in comparison to the current setting, and larger plateau time points ($T = 7$ and 8). More details about these setting are given in Table 1 of the Supplementary File.

Table 3: The posterior median value (standard deviation) of the annual factor level and the turning point α .

Method	Start	1st year	2nd year
Selection	26.93 (1.77)	39.59 (2.96)	35.20 (2.64)
Combination	26.89 (1.68)	40.31 (2.96)	35.87 (2.41)
No-borrow	26.45 (1.67)	40.80 (3.10)	35.14 (2.34)
3rd year	4th year	5th year	α
33.75 (2.87)	32.60 (3.15)	31.94 (3.64)	1.93 (0.09)
33.68 (3.21)	32.26 (3.19)	31.40 (3.09)	2.01 (0.06)
29.58 (3.79)	20.90 (9.92)	12.47 (17.80)	2.07 (0.07)

As shown in Figure 5(c) and (d), the credible bands exhibit a substantial amount of agreement, which confirms a satisfactory level of robustness, i.e., the results obtained are not sensitive to the choice of the hyperparameter values and plateau time points. We have also conducted a residual diagnosis analysis and explored the use of heavy-tailed residuals in the model, with results presented in Sections 3 and 4 of the Supplementary File.

6 Discussion

In this paper, we propose BASE, a data integration method using Bayesian procedures. Our work stands out as the first work that selects subsets from external datasets based on theoretically supported motivations. Compared to the direct combination method, our approach exhibits extra flexibility and interpretability, providing inspiring scientific evidence for future clinical studies. Of note, our work does not intend to provide a definite answer on the long term efficacy of HEMGENIX, but rather showcase a conceptually novel procedure that manages to refine the long-term efficacy inference. As more data from ongoing clinical trials are available, the predicted values may be updated with the same Bayesian approach. For instance, the factor level on the 15-th year post treatment can be predicted if the trials continue, rendering more available durability data.

Despite these achievements, the current model can be generalized in future studies. Firstly, the current MCMC sampling scheme relies on the proposal of the external subset \mathcal{C} . Although the current proposal has a satisfactory empirical performance in simulations and real data analysis, e.g., the standard deviation of the external proportion is moderate compared to the point estimate, it remains unexplored whether this proposal is effective when the external data size is large, for instance, over 100 observations. Intuitively, a more effective proposal should be devised in such scenarios, given that the number of possible external subsets increases at an exponential order with the external data size. However, since the size of the hemophilia external data is manageable (10 observations), this question is beyond the scope of this work. Additionally, the estimation of the marginal likelihood can be further investigated. The current strategy (Pajor, 2017) is proven to be effective under the parametric setting, whilst there is limited evidence that this method provides efficient Monte Carlo estimation to the marginal likelihood under the nonparametric setting. Moreover, when the sample size is sufficiently large, one can consider data-driven strategies that select models from a family of parametric models. Criteria such as the Akaike Information Criterion (AIC; Akaike (1974)), Bayesian Information Criterion (BIC; Schwarz (1978)), and marginal likelihood can be employed to explore if any alternatives are superior in capturing the mean trend compared to the Hermite spline specification. Another intriguing future topic is how to embed the spirit of data selection into non-likelihood problems, e.g., treatment effects that are given by estimating equations and non-probability samples (Yang et al., 2020; Chen et al., 2020). In cases where likelihood functions are not well-defined, it would be impossible to use the marginal likelihood as a guideline, rendering our current pipeline unsuitable. Furthermore, it is also challenging to determine whether the internal estimation benefits from the external data selection.

References

- Akaike, H. (1974). A new look at the statistical model identification. *IEEE transactions on automatic control* 19(6), 716–723.
- Athey, S., R. Chetty, G. W. Imbens, and H. Kang (2019). The surrogate index: Combining short-term proxies to estimate long-term treatment effects more rapidly and precisely. Technical report, National Bureau of Economic Research.
- Cai, T., T. T. Cai, and A. Zhang (2016). Structured matrix completion with applications to genomic data integration. *Journal of the American Statistical Association* 111(514), 621–633.
- Chen, M.-H., J. G. Ibrahim, and Q.-M. Shao (2000). Power prior distributions for generalized linear models. *Journal of Statistical Planning and Inference* 84(1-2), 121–137.
- Chen, M.-H., J. G. Ibrahim, and C. Yiannoutsos (1999). Prior elicitation, variable selection and bayesian computation for logistic regression models. *Journal of the Royal Statistical Society: Series B (Statistical Methodology)* 61(1), 223–242.
- Chen, S., B. Zhang, and T. Ye (2021). Minimax rates and adaptivity in combining experimental and observational data. *arXiv preprint arXiv:2109.10522*.
- Chen, Y., P. Li, and C. Wu (2020). Doubly robust inference with nonprobability survey samples. *Journal of the American Statistical Association* 115(532), 2011–2021.
- Dai, X. and L. Li (2022). Orthogonalized kernel debiased machine learning for multimodal data analysis. *Journal of the American Statistical Association*, 1–15.
- Farmer, C., E. Nikram, L. A. Trigg, S. Robinson, J. Coppell, M. Muthukumar, G. Melendez-Torres, and E. C. Wilson (2023). Etranacogene dezaparvovec for treating moderately severe or severe haemophilia b. *National Institute for Health and Care Excellence*.
- George, L. A., S. K. Sullivan, A. Giermasz, J. E. Rasko, B. J. Samelson-Jones, J. Ducore, A. Cuker, L. M. Sullivan, S. Majumdar, J. Teitel, et al. (2017). Hemophilia b gene therapy with a high-specific-activity factor ix variant. *New England Journal of Medicine* 377(23), 2215–2227.
- Ghosal, S., J. K. Ghosh, and A. W. Van Der Vaart (2000). Convergence rates of posterior distributions. *Annals of Statistics*, 500–531.
- Gomez, E., A. Giermasz, G. Castaman, N. Key, S. Lattimore, F. Leebeek, W. Miesbach, M. Recht, A. Drygalski, E. Sawyer, and S. Pipe (2021). Etranacogene dezaparvovec (aav5-padua hfix variant, amt-061), an enhanced vector for gene transfer in adults with severe or moderate-severe hemophilia B: 2.5 year data from a phase 2b trial. *ISTH Congress*.
- Hassler, G. W., A. F. Magee, Z. Zhang, G. Baele, P. Lemey, X. Ji, M. Fourment, and M. A. Suchard (2023). Data integration in bayesian phylogenetics. *Annual Review of Statistics and Its Application* 10.
- Hector, E. C. and R. Martin (2022). Turning the information-sharing dial: efficient inference from different data sources. *arXiv preprint arXiv:2207.08886*.

- Ibrahim, J. G., M.-H. Chen, Y. Gwon, and F. Chen (2015). The power prior: theory and applications. *Statistics in medicine* 34(28), 3724–3749.
- Imbens, G., N. Kallus, X. Mao, and Y. Wang (2022). Long-term causal inference under persistent confounding via data combination. *arXiv preprint arXiv:2202.07234*.
- Kee, A. and V. Maio (2019). Value-based contracting: challenges and opportunities. *American Journal of Medical Quality* 34(6), 615–617.
- Leebeek, F. W. and W. Miesbach (2021). Gene therapy for hemophilia: a review on clinical benefit, limitations, and remaining issues. *Blood* 138(11), 923–931.
- Li, Q. and L. Li (2022). Integrative factor regression and its inference for multimodal data analysis. *Journal of the American Statistical Association* 117(540), 2207–2221.
- Li, S. and A. Luedtke (2021). Efficient estimation under data fusion. *arXiv preprint arXiv:2111.14945*.
- Liu, Y., X. Sun, W. Zhong, and B. Li (2022). B-scaling: A novel nonparametric data fusion method. *The Annals of Applied Statistics* 16(3), 1292–1312.
- Miesbach, W., K. Meijer, M. Coppens, P. Kampmann, R. Klamroth, R. Schutgens, G. Castaman, S. E.K, and L. F.WG (2021). Five year data confirms stable fix expression and sustained reductions in bleeding and factor ix use following amt-060 gene therapy in adults with severe or moderate-severe hemophilia B. *ISTH Congress*.
- Nathwani, A. C., U. Reiss, E. Tuddenham, P. Chowdary, J. McIntosh, A. Riddell, J. Pie, J. N. Mahlangu, M. Recht, Y.-M. Shen, K. G. Halka, M. M. Meagher, A. W. Nienhuis, A. M. Davidoff, S. Mangles, C. L. Morton, Z. Junfang, and V. C. Radulescu (2018, 11). Adeno-associated mediated gene transfer for hemophilia B:8 year follow up and impact of removing "empty viral particles" on safety and efficacy of gene transfer. *Blood* 132(Supplement 1), 491–491.
- Nathwani, A. C., U. M. Reiss, E. G. Tuddenham, C. Rosales, P. Chowdary, J. McIntosh, M. Della Peruta, E. Lheriteau, N. Patel, D. Raj, et al. (2014). Long-term safety and efficacy of factor ix gene therapy in hemophilia B. *New England Journal of Medicine* 371(21), 1994–2004.
- Nathwani, A. C., E. G. Tuddenham, S. Rangarajan, C. Rosales, J. McIntosh, D. C. Linch, P. Chowdary, A. Riddell, A. J. Pie, C. Harrington, et al. (2011). Adenovirus-associated virus vector-mediated gene transfer in hemophilia B. *New England Journal of Medicine* 365(25), 2357–2365.
- Neuenschwander, B., M. Branson, and D. J. Spiegelhalter (2009). A note on the power prior. *Statistics in medicine* 28(28), 3562–3566.
- Oberst, M., A. D’Amour, M. Chen, Y. Wang, D. Sontag, and S. Yadlowsky (2022). Bias-robust integration of observational and experimental estimators. *arXiv preprint arXiv:2205.10467*.
- Pajor, A. (2017). Estimating the marginal likelihood using the arithmetic mean identity.
- Park, S., H. Xu, and H. Zhao (2021). Integrating multidimensional data for clustering analysis with applications to cancer patient data. *Journal of the American Statistical Association* 116(533), 14–26.

- Pipe, S. W., F. W. Leebeek, M. Recht, N. S. Key, G. Castaman, W. Miesbach, S. Lattimore, K. Peerlinck, P. Van der Valk, M. Coppens, et al. (2023). Gene therapy with etranacogene dezaparvovec for hemophilia B. *New England Journal of Medicine* 388(8), 706–718.
- Ritchie, M. D., E. R. Holzinger, R. Li, S. A. Pendergrass, and D. Kim (2015). Methods of integrating data to uncover genotype–phenotype interactions. *Nature Reviews Genetics* 16(2), 85–97.
- Robert, C. P. et al. (2007). *The Bayesian choice: from decision-theoretic foundations to computational implementation*, Volume 2. Springer.
- Samelson-Jones, B. J., S. K. Sullivan, J. E. Rasko, A. Giermasz, L. A. George, J. M. Ducore, J. M. Teitel, C. E. McGuinn, A. O’Brien, I. Winburn, et al. (2021). Follow-up of more than 5 years in a cohort of patients with hemophilia b treated with fidanacogene elaparvovec adeno-associated virus gene therapy. *Blood* 138, 3975.
- Schwarz, G. (1978). Estimating the dimension of a model. *The annals of statistics*, 461–464.
- Shah, J., H. Kim, K. Sivamurthy, P. E. Monahan, and M. Fries (2023). Comprehensive analysis and prediction of long-term durability of factor ix activity following etranacogene dezaparvovec gene therapy in the treatment of hemophilia B. *Current Medical Research and Opinion* 39(2), 227–237.
- Shen, W., S. T. Tokdar, and S. Ghosal (2013). Adaptive bayesian multivariate density estimation with dirichlet mixtures. *Biometrika* 100(3), 623–640.
- Tice, J., S. Walton, B. Herce-Hagiwara, S. Fahim, A. Moradi, J. Sarker, J. Chu, F. Agboola, S. Pearson, and D. Rind (2022, 12). Gene therapy for hemophilia B and an update on gene therapy for hemophilia A: Effectiveness and value. *Institute for Clinical and Economic Review*.
- Valentinuzzi, M. E. (2004). Friedman lm, furberg cd, demets dl: Fundamentals of clinical trials 3rd edition: Springer-verlag, new york; 1998. 361 pp, isbn 0-387-98586-7.
- Xue, F. and A. Qu (2021). Integrating multisource block-wise missing data in model selection. *Journal of the American Statistical Association* 116(536), 1914–1927.
- Yang, S., C. Gao, D. Zeng, and X. Wang (2020). Elastic integrative analysis of randomized trial and real-world data for treatment heterogeneity estimation. *arXiv preprint arXiv:2005.10579*.
- Yang, S., J. K. Kim, and R. Song (2020). Doubly robust inference when combining probability and non-probability samples with high dimensional data. *Journal of the Royal Statistical Society. Series B, Statistical Methodology* 82(2), 445.